Electronic Supplementary Material (ESI) for Chemical Science.

Supporting Information for

Outer-sphere effects on ligand-field excited-state dynamics: solvent dependence of high-spin to low-spin conversion in $[Fe(bpy)_3]^{2+}$

Jennifer N. Miller[a] and James K. McCusker[b]*

Contribution from the Department of Chemistry, Michigan State University

578 South Shaw Lane East Lansing, Michigan 48824 USA

[a]Email address: mill1985@msu.edu

[b]Email address: jkm@chemistry.msu.edu

Table of Contents

List of Figures and Tables

Experimental Section

Syntheses and Characterization of Fe(II) Complexes. All of the following complexes were prepared under an inert atmosphere. In general, 1 equivalent of the Fe(II) source was dissolved in nitrogen-sparged water and transferred via cannula to a flask containing 3.1 equivalents of the ligand dissolved in air-free methanol, resulting in a red-colored solution. 10 equivalents of the anion source, dissolved in bubble-degassed water, were cannula-transferred to the reaction flask, after which the reaction mixture was allowed to stir for 2 hours. Any modifications to this procedure are noted in the appropriate section. Purification methods are described individually.

Tris(2,2'-bipyridine)iron(II) chloride, [Fe(bpy)$_3$]Cl$_2$. This complex was prepared by a previous group member, Amanda Smeigh, in a N_2-filled glovebox by mixing $FeCl_2{\cdot}2H_2O$ and 2,2'-bipyridine in methanol. No water was used in this reaction. The solution was allowed to stir for 10 minutes at room temperature. After evaporating the solvent under a stream of nitrogen, the product was recrystallized via diethyl ether vapor diffusion into a saturated acetonitrile solution of the complex. ^{1}H NMR (CD_3CN, 500 MHz): δ 8.57 (d, 6H, J = 8 Hz), 8.10 (m, 6H), 7.40 (m, 12H). TOF-MS [ESI, *m/z*]: 262.07 $[C_{30}H_{24}N_6Fe]^{2+}$. Elemental Analysis for $C_{30}H_{24}N_6FeCl_2{\cdot}2H_2O$, Calculated: C, 57.07%; H, 4.47%; N, 13.31%. Found: C, 57.15%; H, 4.33%; N, 13.32%. UV-Vis (CH_3CN) λ (ε($M^{-1}cm^{-1}$)): 298 nm (55600), 350 (5700), 521 (6900).

Tris(2,2'-bipyridine)iron(II) bromide, [Fe(bpy)$_3$]Br$_2$. This complex was prepared on a Schlenk line, under air-free conditions. $(NH_4)_2Fe(SO_4)_2{\cdot}6H_2O$, 2,2'-bipyridine, and NaBr were the starting materials for this reaction. Following 2 hours of stirring, the solvent was removed from the reaction mixture by a rotary evaporator. The crude product was dissolved in acetonitrile and filtered. The filtrate was then recrystallized by diethyl ether vapor diffusion into a saturated acetonitrile solution of the complex. The last two steps were repeated. ^{1}H NMR (CD_3CN, 500 MHz): δ 8.55 (d, 6H, J = 8 Hz), 8.11 (m, 6H), 7.39 (m, 12H). TOF-MS [ESI, *m/z*]: 262.07 $[C_{30}H_{24}N_6Fe]^{2+}$. Elemental Analysis for $C_{30}H_{24}N_6FeBr_2{\cdot}3H_2O$, Calculated: C, 48.81%; H, 4.10%; N, 11.38%. Found: C, 48.79%; H, 4.04%; N, 11.80%. UV-Vis (CH_3CN) λ (ε($M^{-1}cm^{-1}$)): 299 nm (60200), 350 nm (5800), 520 nm (7800).

Tris(2,2'-bipyridine)iron(II) iodide, [Fe(bpy)$_3$]I$_2$. This complex was prepared on a Schlenk line, under air-free conditions. $(NH_4)_2Fe(SO_4)_2{\cdot}6H_2O$, 2,2'-bipyridine, and NaI made up the reactants. Some of the crude product from this reaction formed a precipitate which was filtered. Under vacuum filtration, the precipitate was rinsed with acetone and diethyl ether. The product was then dissolved in acetonitrile, filtered, and recrystallized twice by diethyl ether vapor diffusion. ^{1}H NMR (CD_3CN, 500 MHz): δ 8.53 (d, 6H, J = 8 Hz), 8.10 (m, 6H), 7.39 (m, 12H). TOF-MS [ESI, *m/z*]: 262.07 $[C_{30}H_{24}N_6Fe]^{2+}$. Elemental Analysis for $C_{30}H_{24}N_6FeI_2{\cdot}2H_2O$, Calculated: C, 44.25%; H, 3.47%; N, 10.32%. Found: C, 45.52%; H, 3.53%; N, 10.36%. UV-Vis (CH_3CN) λ (ε($M^{-1}cm^{-1}$)): 298 nm (64900), 351 nm (6500), 520 nm (8400).

Tris(2,2'-bipyridine)iron(II) hexafluorophosphate, [Fe(bpy)$_3$](PF$_6$)$_2$. This complex was prepared on a Schlenk line, under air-free conditions. The reaction mixture contained $(NH_4)_2Fe(SO_4)_2{\cdot}6H_2O$, 2,2'-bipyridine, and NH_4PF_6. The product precipitated out upon the addition of NH_4PF_6. The solid product was filtered and rinsed with water, then diethyl ether. The product was then dissolved in acetonitrile, filtered, and recrystallized twice by diethyl ether vapor diffusion. ^{1}H NMR (CD_3CN, 500 MHz): δ 8.51 (d, 6H, J = 8 Hz), 8.10 (m, 6H), 7.38 (m, 12H).

TOF-MS [ESI, *m/z*]: 262.07 $[C_{30}H_{24}N_6Fe]^{2+}$. Elemental Analysis for $C_{30}H_{24}N_6FeP_2F_{12}$, Calculated: C, 44.25%; H, 2.97%; N, 10.32%. Found: C, 44.23%; H, 3.03%; N, 10.32%. UV-Vis (CH_3CN) λ (ε($M^{-1}cm^{-1}$)): 299 nm (69500), 351 nm (6700), 520 nm (9100).

Tris(2,2'-bipyridine)iron(II) tetraphenylborate, [Fe(bpy)$_3$](BPh$_4$)$_2$. This complex was prepared on a Schlenk line, under air-free conditions. It was prepared from $FeCl_2{\cdot}2H_2O$, 2,2'-bipyridine, and $NaBPh_4$. The product formed a precipitate which was filtered and rinsed with water and diethyl ether. The product was then dissolved in acetone, filtered, and recrystallized twice by diethyl ether vapor diffusion. ^{1}H NMR (CD_3CN, 500 MHz): δ 8.49 (d, 6H, *J* = 8Hz), 8.08 (td, 6H, *J* = 7.5, 2 Hz), 7.37 (m, 12H), 7.26 (m, 16H), 6.98 (t, 16H, *J* = 7.3), 6.83 (t, 8H, *J* = 7.3). TOF-MS [ESI, *m/z* (rel. int.)]: 262.07 (100) $[C_{30}H_{24}N_6Fe]^{2+}$, 843.31 (13) $\{[C_{30}H_{24}N_6Fe](C_{24}H_{20}B)\}^+$. Elemental Analysis for $C_{78}H_{64}N_6FeB_2{\cdot}H_2O$, Calculated: C, 79.34%; H, 5.63%; N, 7.12%. Found: C, 79.48%; H, 5.85%; N, 6.90%. UV-Vis (CH_3CN) λ (ε($M^{-1}cm^{-1}$)): 299 nm (68200), 351 nm (6600), 520 nm (8900).

Tris(2,2'-bipyridine)iron(II) tetrakis(3,5-bis(trifluoromethyl)phenyl)borate, [Fe(bpy)$_3$](BAr$^F_4$)$_2$. This complex was prepared on a Schlenk line, under air-free conditions, starting from $(NH_4)_2Fe(SO_4)_2{\cdot}6H_2O$, 2,2'-bipyridine, and 2.10 equivalents of $NaBAr^F_4$. The product precipitated from the solution and was subsequently filtered. Under vacuum filtration, the product was dissolved in diethyl ether and filtered. The product was precipitated out of the filtrate by adding acetone. The last two steps were repeated. ^{1}H NMR (CD_3CN, 500 MHz): δ 8.50 (d, 6H, *J* = 7.5 Hz), 8.10 (m, 6H), 7.69 (m, 16H), 7.66 (s, 8H), 7.38 (m, 12H). TOF-MS [ESI, *m/z* (rel. int.)]: 262.07 (100) $[C_{30}H_{24}N_6Fe]^{2+}$, 1387.22 (40) $\{[C_{30}H_{24}N_6Fe](C_{32}H_{12}BF_{24})\}^+$. Elemental Analysis for $C_{94}H_{48}N_6FeB_2F_{48}{\cdot}2H_2O$, Calculated: C, 49.37%; H, 2.29%; N, 3.67%. Found: C, 50.21%; H, 2.36%; N, 3.60%. UV-Vis (CH_3CN) λ (ε($M^{-1}cm^{-1}$)): 299 nm (64900), 351 nm (6300), 521 nm (8400).

Tris(4,4'-dimethyl-2,2'-bipyridine)iron(II) bromide, [Fe(dmb)$_3$]Br$_2$. This complex was prepared on a Schlenk line, under air-free conditions. $[Fe(dmb)_3]Br_2$ was synthesized from $(NH_4)_2Fe(SO_4)_2{\cdot}6H_2O$, 4,4'-dimethyl-2,2'-bipyridine, and NaBr. After allowing the reaction to stir for 2 hours, the solvent was removed by a rotary evaporator. The crude product was dissolved in acetonitrile and filtered. The product was crashed out of the filtrate with diethyl ether. The solid product was collected by vacuum filtration. The last three steps were repeated. Allowing the sample to recrystallize in diethyl ether led to the solution developing an orange tint. ^{1}H NMR (CD_3CN, 500 MHz): δ 8.37 (s, 6H), 7.19 (m, 12H), 2.53 (s, 18H). TOF-MS [ESI, *m/z* (rel. int.)]: 212.07 (61) $[C_{24}H_{24}N_4Fe]^{2+}$, 304.12 (100) $[C_{36}H_{36}N_6Fe]^{2+}$, 503.05 (41) $\{[C_{24}H_{24}N_4Fe]Br\}^+$. Elemental Analysis for $C_{36}H_{36}N_6FeBr_2{\cdot}H_2O$, Calculated: C, 54.98%; H, 4.87%; N, 10.69%. Found: C, 54.29%; H, 4.72%; N, 10.63%. UV-Vis (CH_3CN) λ (ε($M^{-1}cm^{-1}$)): 297 nm (64300), 356 nm (7300), 527 nm (8500).

Tris(5,5'-dimethyl-2,2'-bipyridine)iron(II) bromide, [Fe(5,5'-dmb)$_3$]Br$_2$. This complex was prepared on a Schlenk line, under air-free conditions. The reagents for this reaction were $(NH_4)_2Fe(SO_4)_2{\cdot}6H_2O$, 5,5'-dimethyl-2,2'-bipyridine, and NaBr. After allowing the reaction to stir for 2 hours, the solvent was removed by a rotary evaporator. The crude product was dissolved in acetonitrile and filtered. The product was recrystallized twice by diethyl ether vapor diffusion into a saturated acetonitrile solution of the complex. ^{1}H NMR (CD_3CN, 500 MHz): δ 8.35 (d, 6H, *J* = 8 Hz), 7.88 (dd, 6H, *J* = 7.8, 1.3 Hz), 7.09 (s, 6H), 2.16 (s, 18H). TOF-MS [ESI, *m/z* (rel. int.)]:

212.07 (47) $[C_{24}H_{24}N_4Fe]^{2+}$, 304.12 (100) $[C_{36}H_{36}N_6Fe]^{2+}$, 503.05 (27) $\{[C_{24}H_{24}N_4Fe]Br\}^{+}$. Elemental Analysis for $C_{36}H_{36}N_6FeBr_2 \cdot H_2O$, Calculated: C, 54.98%; H, 4.87%; N, 10.69%. Found: C, 54.81%; H, 5.11%; N, 10.58%. UV-Vis (CH_3CN) λ (ε($M^{-1}cm^{-1}$)): 306 nm (78700), 355 nm (6500), 510 nm (9400).

Tris(4,4'-di-tert-butyl-2,2'-bipyridine)iron(II) bromide, [Fe(dtbbpy)$_3$]Br$_2$. This complex was prepared on a Schlenk line, under air-free conditions. $(NH_4)_2Fe(SO_4)_2 \cdot 6H_2O$, 4,4'-di-*tert*-butyl-2,2'-bipyridine and NaBr were the starting materials for this reaction. After stirring for 2 hours, the solvent was removed from the reaction mixture by a rotary evaporator. The crude product was dissolved in acetonitrile and filtered. The filtrate was then recrystallized twice by diethyl ether vapor diffusion into a saturated acetonitrile solution of the complex. ^{1}H NMR (CD_3CN, 500 MHz): δ 8.51 (d, 6H, J = 2.0 Hz), 7.39 (dd, 6H, J = 6.0, 2.0 Hz), 7.20 (d, 6H, J = 6.0 Hz), 1.41 (s, 54H). TOF-MS [ESI, *m/z*]: 430.26 $[C_{54}H_{72}N_6Fe]^{2+}$. Elemental Analysis for $C_{54}H_{72}N_6FeBr_2$, Calculated: C, 63.53%; H, 7.11%; N, 8.23%. Found: C, 63.35%; H, 6.84%; N, 8.34%. UV-Vis (CH_3CN) λ (ε($M^{-1}cm^{-1}$)): 298 nm (67300), 357 nm (8500), 527 nm (10200).

Ground State Electronic Absorption Spectra.

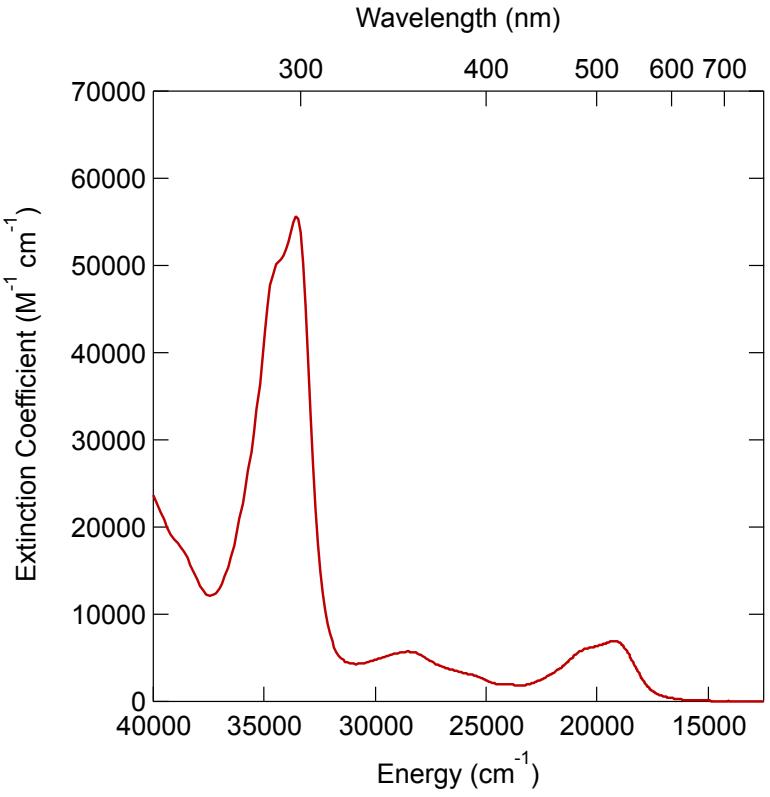

Figure S1. Electronic absorption spectrum of $[Fe(bpy)_3]Cl_2$ in acetonitrile.

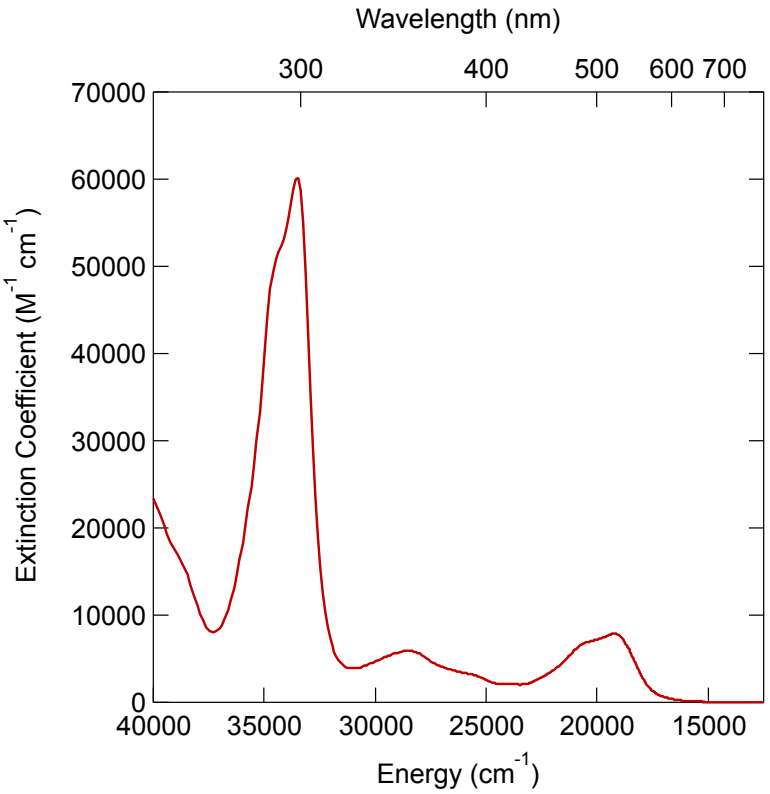

Figure S2. Electronic absorption spectrum of $[Fe(bpy)_3]Br_2$ in acetonitrile.

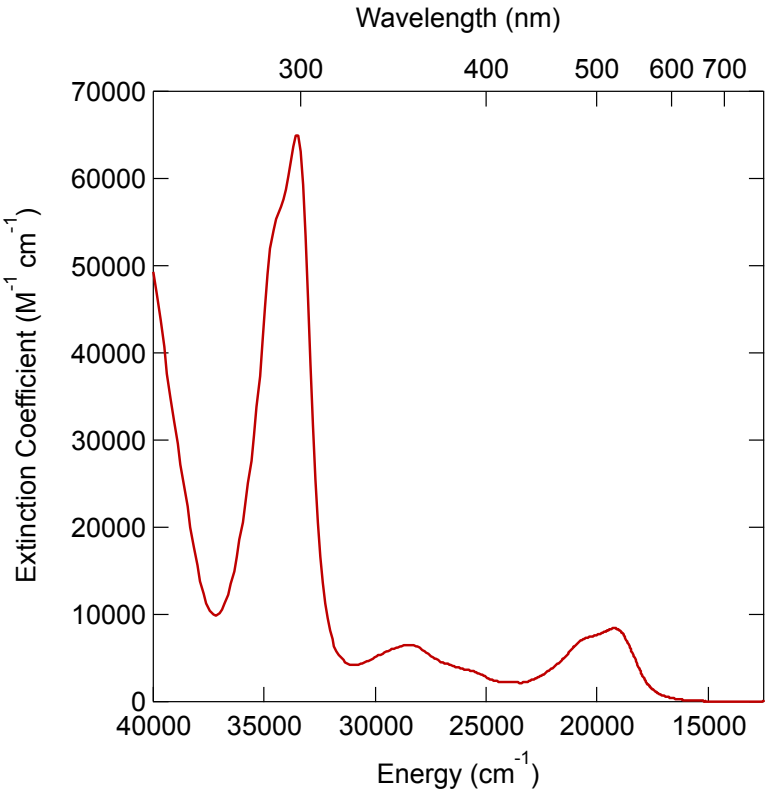

Figure S3. Electronic absorption spectrum of $[Fe(bpy)_3]I_2$ in acetonitrile.

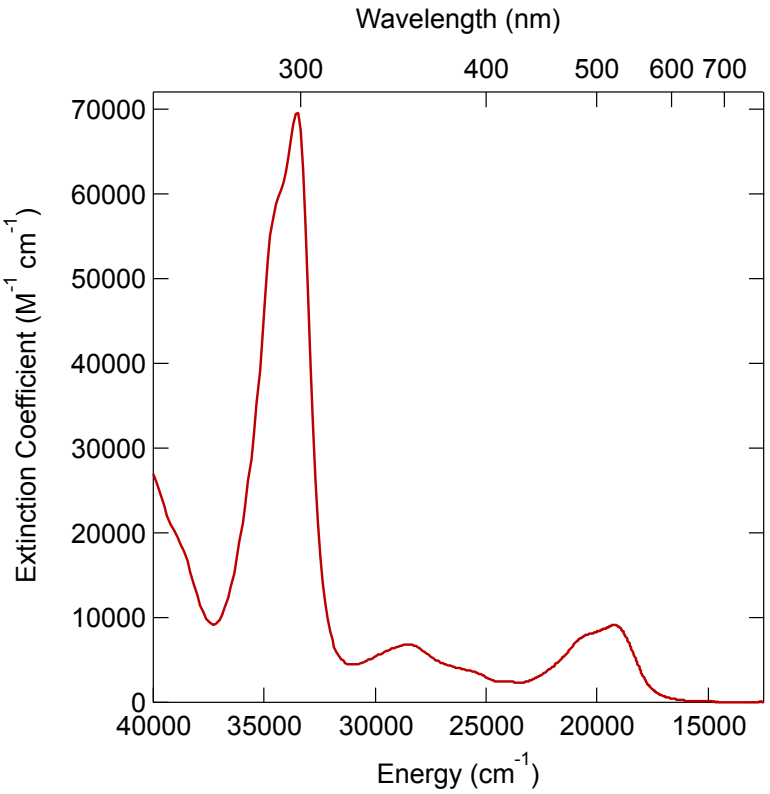

Figure S4. Electronic absorption spectrum of $[Fe(bpy)_3](PF_6)_2$ in acetonitrile.

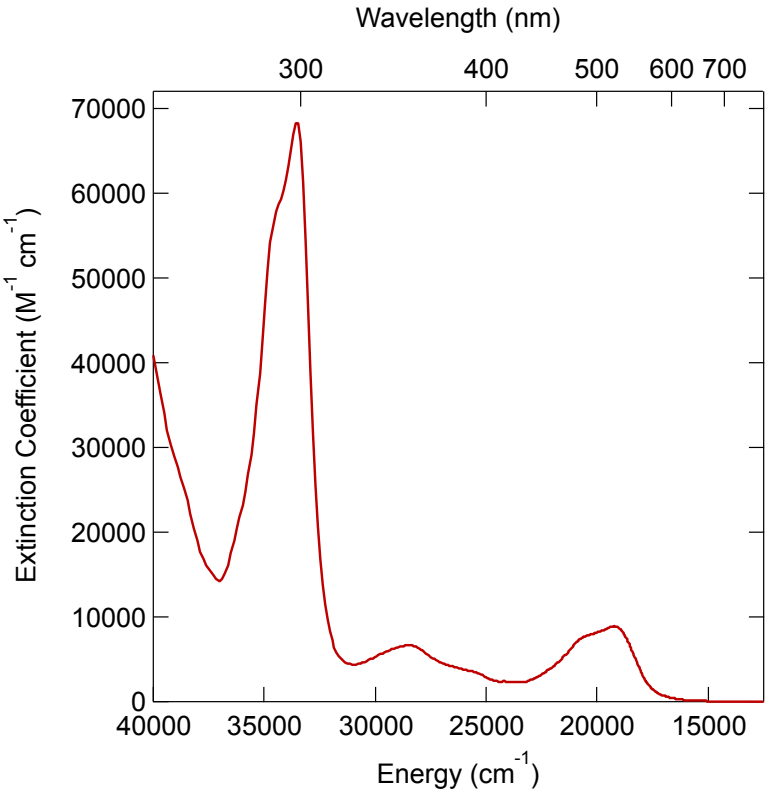

Figure S5. Electronic absorption spectrum of $[Fe(bpy)_3](BPh_4)_2$ in acetonitrile.

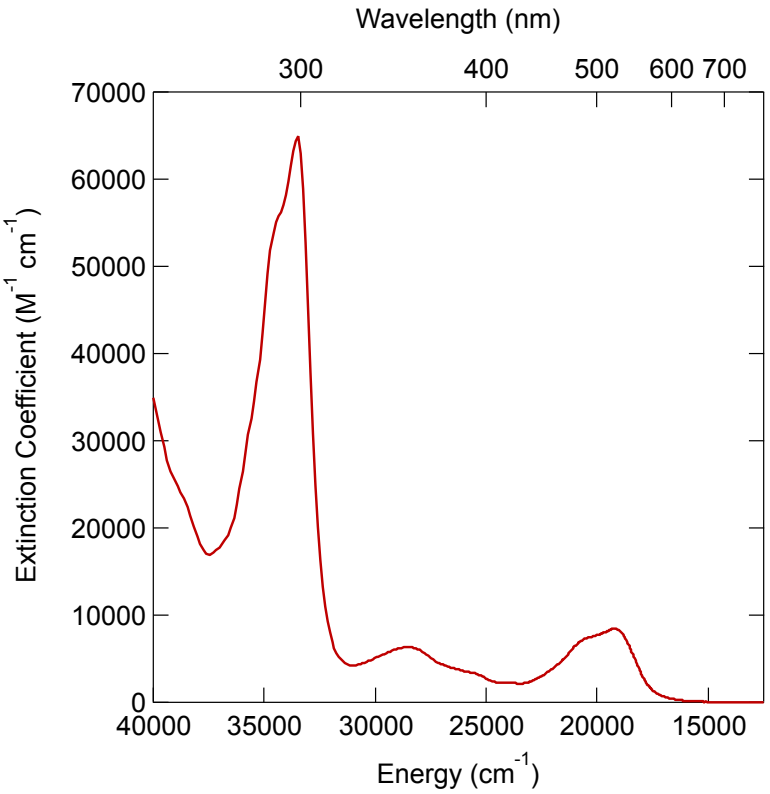

Figure S6. Electronic absorption spectrum of $[Fe(bpy)_3](BAr^F{}_4)_2$ in acetonitrile.

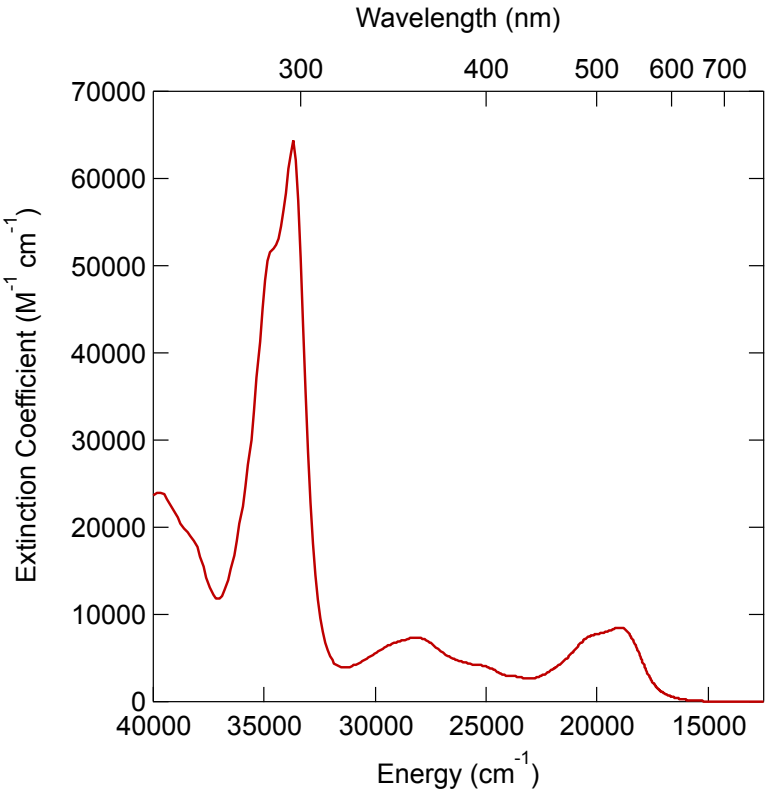

Figure S7. Electronic absorption spectrum of $[Fe(dmb)_3]Br_2$ in acetonitrile.

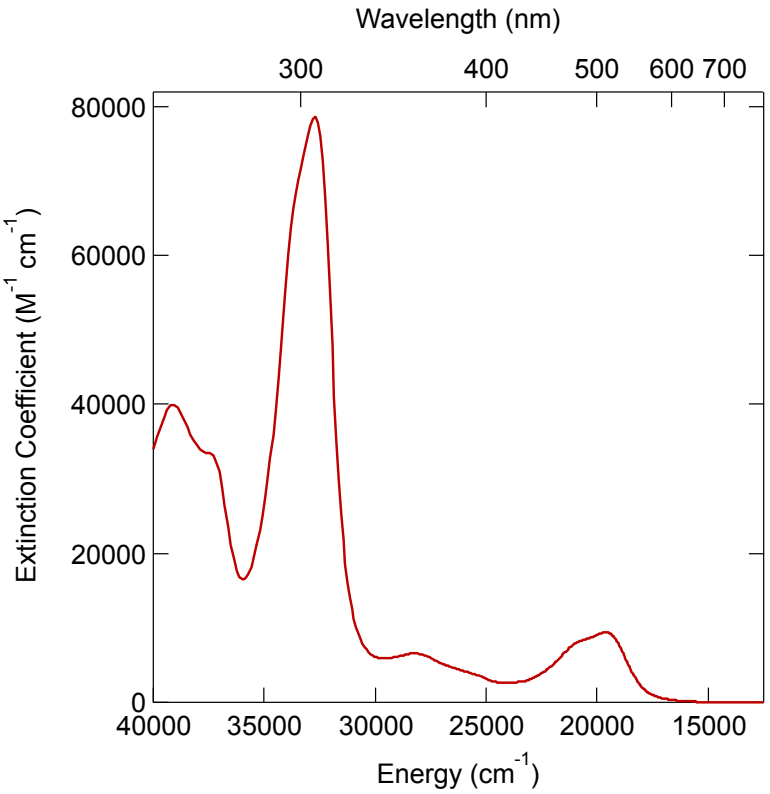

Figure S8. Electronic absorption spectrum of $[Fe(5,5'\text{-dmb})_3]Br_2$ in acetonitrile.

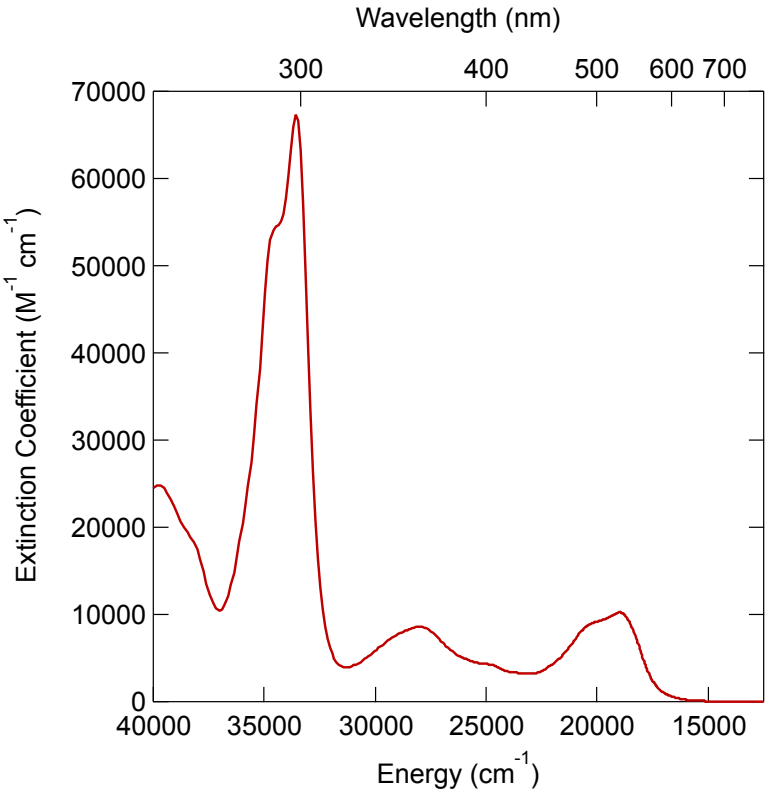

Figure S9. Electronic absorption spectrum of $[Fe(dtbbpy)_3]Br_2$ in acetonitrile.

Ultrafast Laser System for Time-Resolved Spectroscopic Measurements.

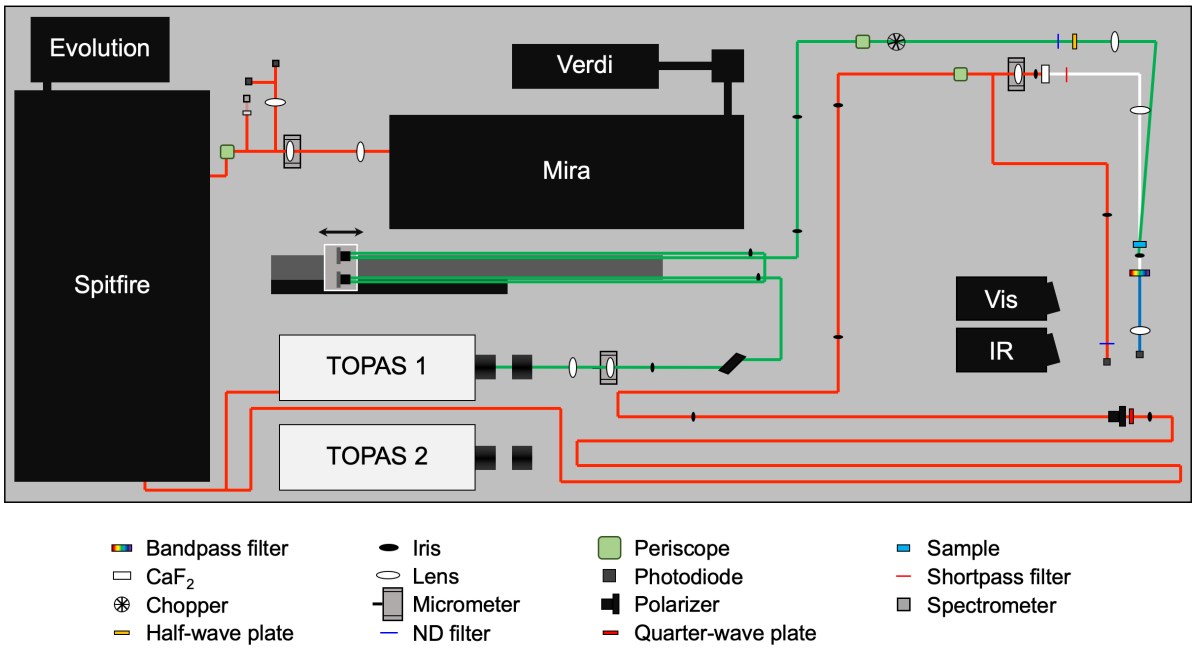

Figure S10. Layout of the ultrafast laser system used in this study. The green beam represents the pump beam line. The red beam bypassing TOPAS 2 is the probe beam which generates a white light continuum in calcium fluoride just before the sample.

Results and Discussion

Correlation of Solvent Properties with Ground State Recovery Lifetimes.

Table S1. Properties associated with each solvent[a,b]

	Dipole Moment (D)	Molar Volume[c] (cm^3/mol)	Optical Dielectric Constant[d]	Polariz-ability[e] (Å^3)	Static Dielectric Constant	Viscosity (cP)
Water	1.85	18.05	1.78	1.47	80.10	0.89
Dimethyl Sulfoxide	3.96	70.97[f]	2.19	7.98[g]	47.24	1.99
Ethylene Glycol	2.36	55.74	2.05	5.73	41.40	16.06
1,3-Propanediol	2.55	72.21	2.07	7.54	35.10	41.11[h]
1,4-Butanediol	2.58	88.60	2.09	9.37	32.86	71.14[h]
1,5-Pentanediol	2.50	105.05	2.10	11.18	26.20	86.79[h]
Propylene Carbonate	4.90	84.74	2.01	8.48	66.14	2.47[i]
Methanol	1.70	40.49	1.77	3.26	33.00	0.54
Ethanol	1.69	58.37	1.85	5.12	25.30	1.07
Acetonitrile	3.93	52.25	1.81[j]	4.39[g]	36.64	0.37
Propionitrile	4.05	70.45	1.86	6.25	29.70	0.29
2-Propanol	1.58	76.95	1.90	7.03	20.18	2.04
Butyronitrile	3.82[k]	87.08	1.92	8.07	24.83	0.55
1-Butanol	1.66	91.56	1.96	8.78	17.84	2.54
Tetrahydrofuran	1.75	81.63[f]	1.97[f]	7.93[f]	7.56	0.46
Hexanenitrile	3.48[l]	120.68	1.98	11.77	17.26[f]	0.91
Diethyl Ether	1.10	103.84	1.83	8.92	4.27	0.22
Dichloromethane	1.60	64.02	2.03	6.48	9.00	0.41
R^2 coefficient[m]	**0.068**	**0.198**	**0.044**	**0.090**	**0.697**	**0.095**

[a]From reference 1, unless otherwise indicated.
[b]All solvent properties but viscosity are based on a temperature of 20 °C, unless noted, with viscosity values established at 25 °C.
[c]Calculated from density (g/cm^3) and molar mass (g/mol).
[d]Calculated from refractive index.
[e]Calculated from refractive index, density (g/cm^3), and molar mass (g/mol).
[f]At 25 °C.
[g]Calculated from data encompassing two different temperatures.
[h]From reference 2.
[i]From reference 3.
[j]At 30 °C.
[k]Average dipole moment between *gauche* (3.91 D) and *anti* (3.73 D) conformers of butyronitrile.
[l]From reference 4.
[m]From linear fit for ground state recovery time constant of $[Fe(bpy)_3]^{2+}$ plotted against that solvent property.

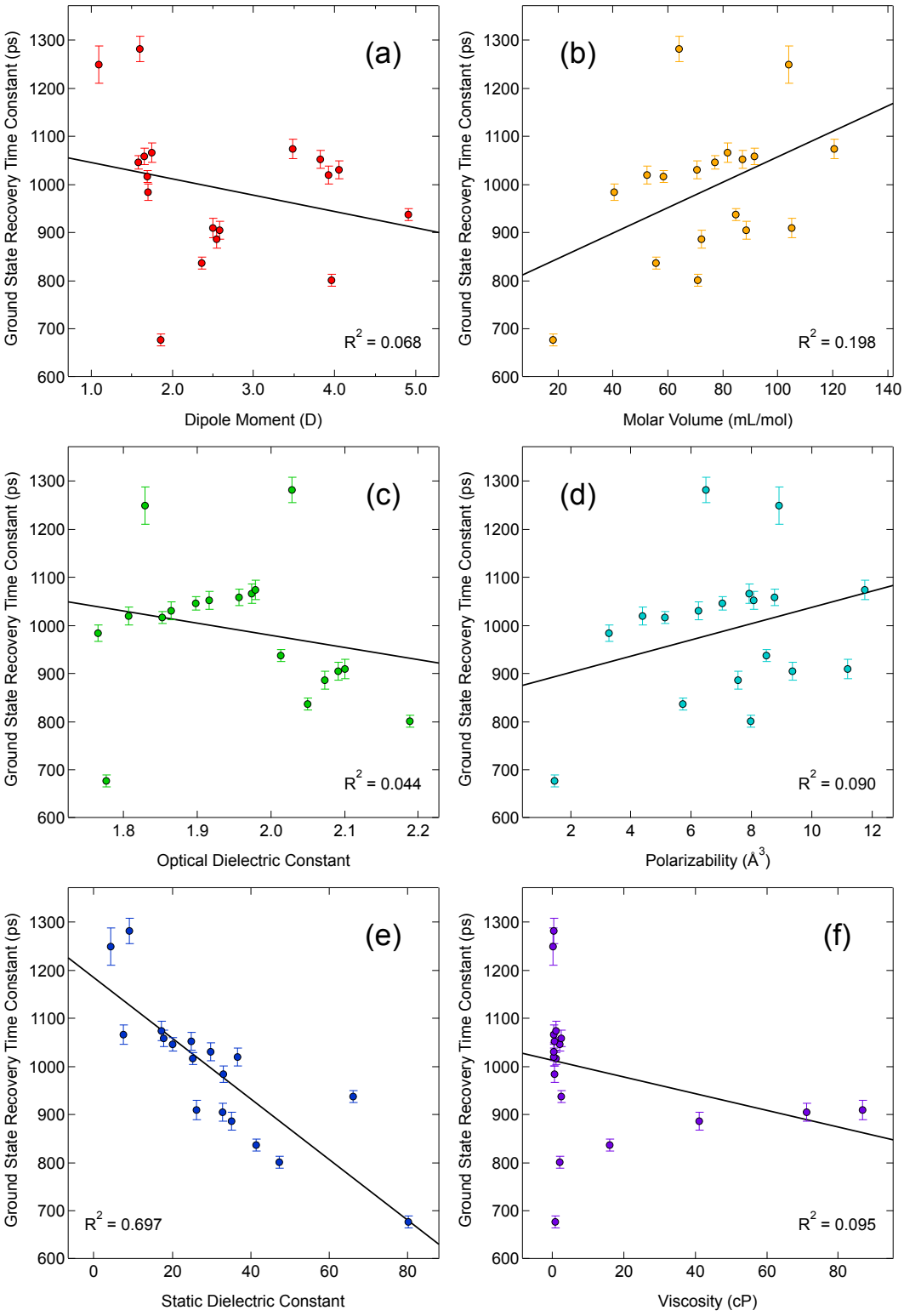

Figure S11. Comparison of ground state recovery lifetime for $[Fe(bpy)_3]^{2+}$ versus (a) dipole moment, (b) molar volume, (c) optical dielectric constant, (d) polarizability, (e) static dielectric constant, and (f) viscosity. The data in (e) is also in the main text, in Figure 2a.

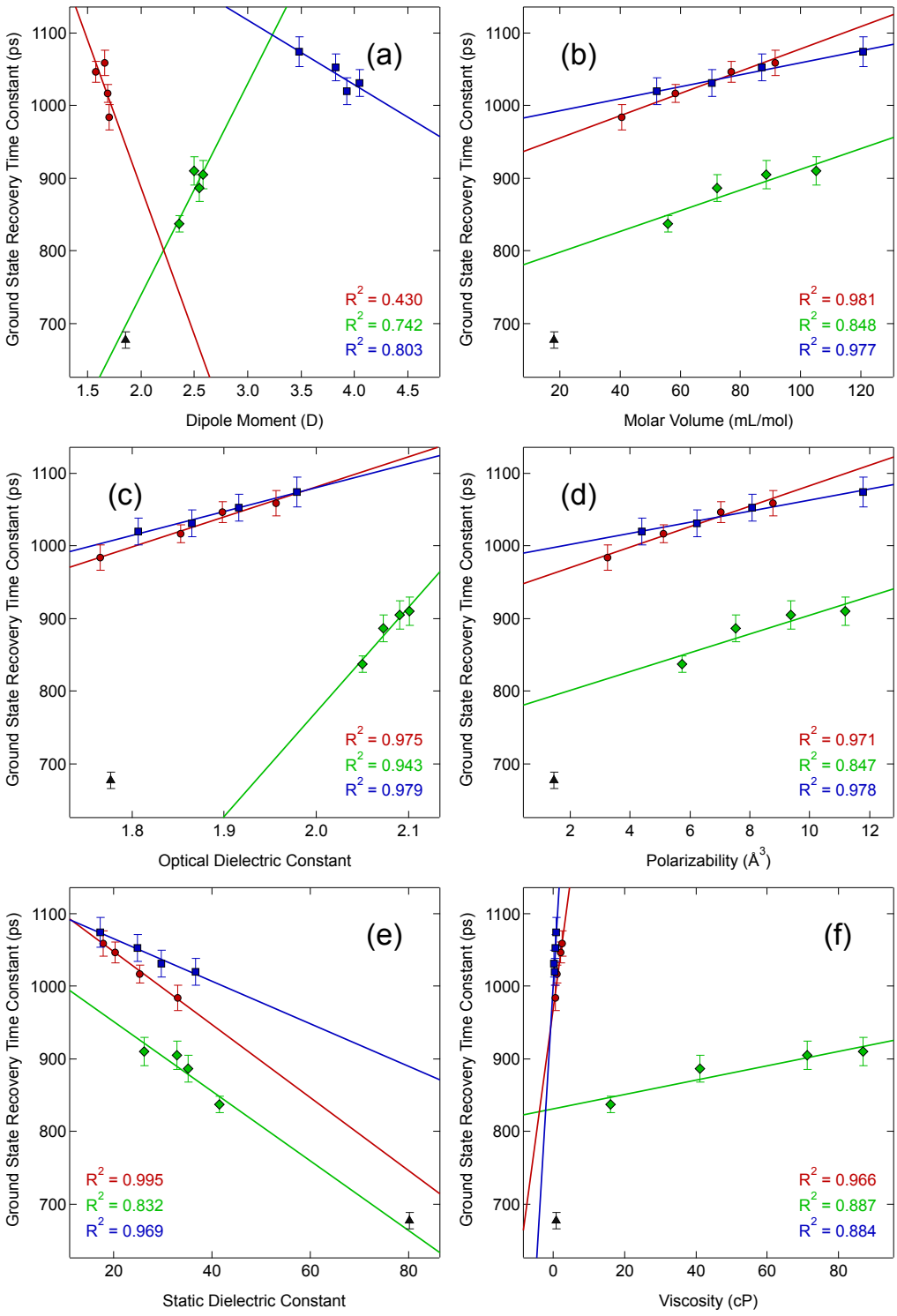

Figure S12. Comparison of ground state recovery lifetime for $[Fe(bpy)_3]^{2+}$ versus (a) dipole moment, (b) molar volume, (c) optical dielectric constant, (d) polarizability, (e) static dielectric constant, and (f) viscosity for alcohols (red circles), diols (green diamonds), and nitriles (blue squares). The results for water (black triangles) are presented in the figures, but are not included in any fits. The data in (e) can also be found in the main text, in Figure 2b.

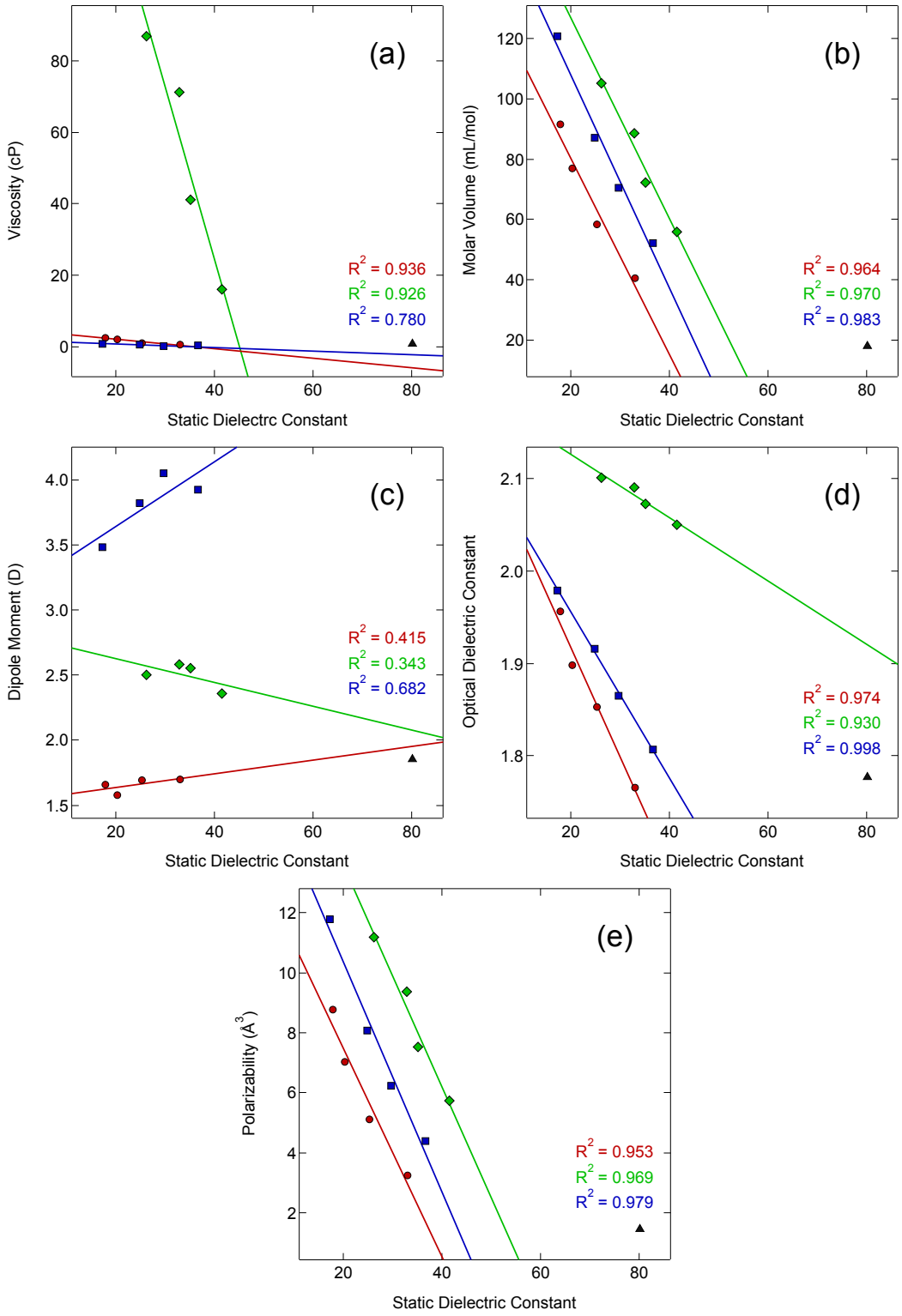

Figure S13. Comparison of the static dielectric constant versus (a) viscosity, (b) molar volume, (c) dipole moment, (d) optical dielectric constant, and (e) polarizability for alcohols (red circles), diols (green diamonds), and nitriles (blue squares). The results for water (black triangles) are presented in the figures, but are not included in any fits.

$[Fe(bpy)_3]^{2+}$ Concentration Studies for Ion Pairing.

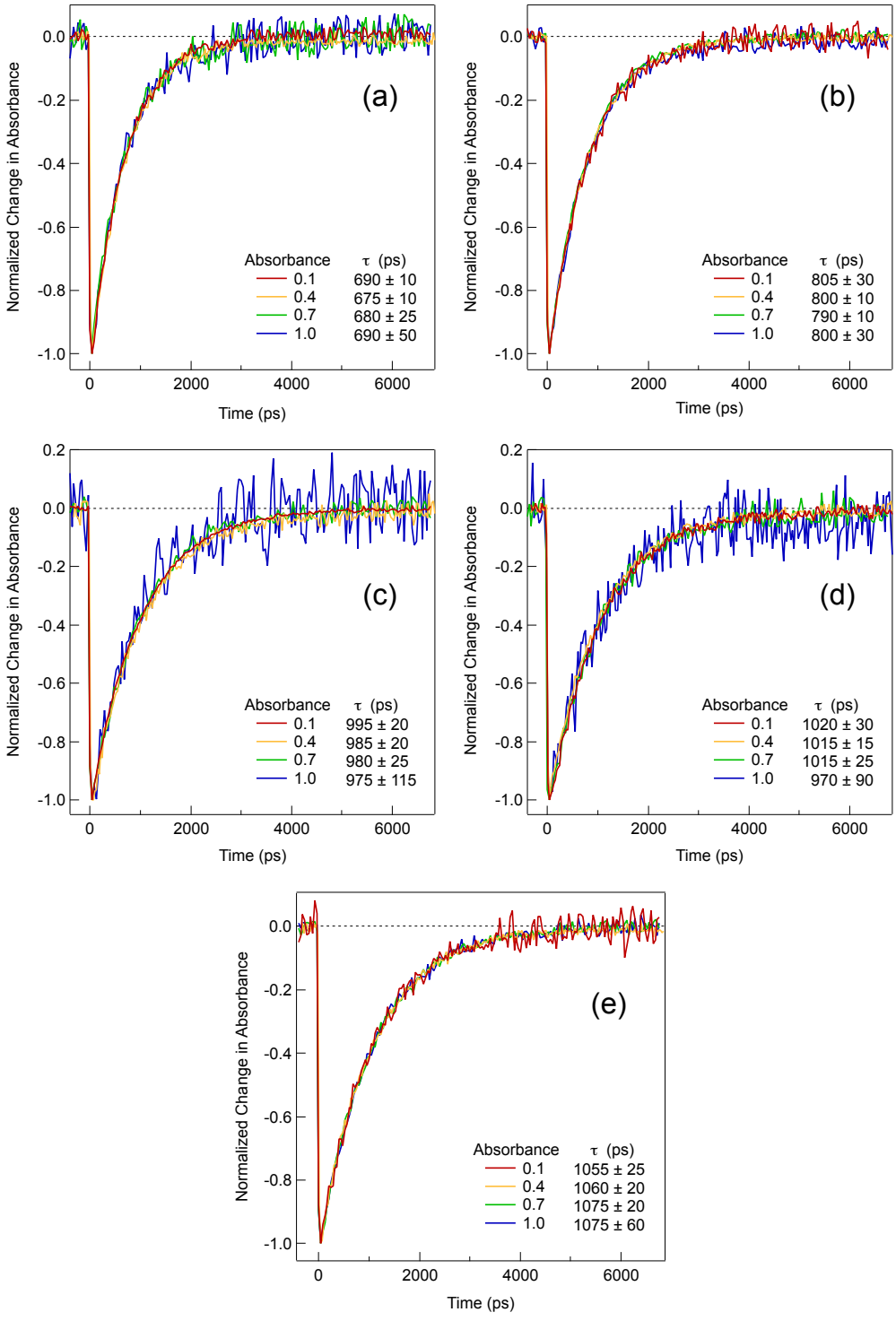

Figure S14. Time constants for ground state recovery of $[Fe(bpy)_3]Br_2$ in (a) water, (b) dimethyl sulfoxide, (c) methanol, (d) acetonitrile, and (e) 1-butanol at different concentrations after excitation at 550 nm. The error associated with each data point has been omitted for clarity.

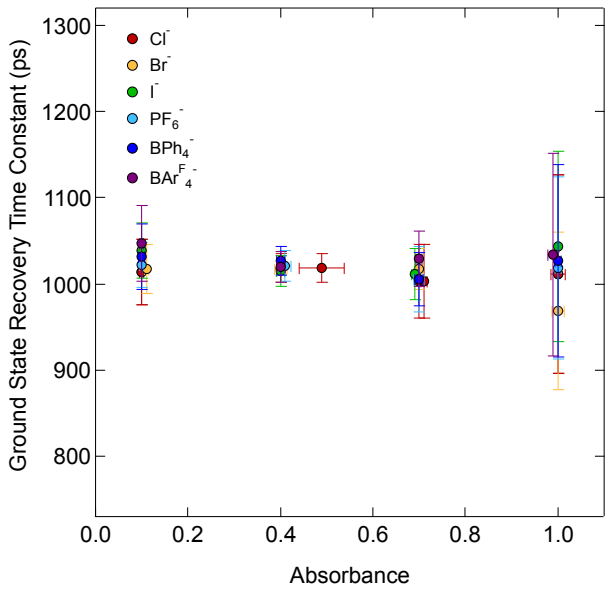

Figure S15. Ground state recovery lifetimes for $[Fe(bpy)_3]^{2+}$ in acetonitrile at different concentrations. Error bars represent the standard deviation of the x- and y-values.

Table S2. Comparison of relaxation times for $[Fe(bpy)_3]^{2+}$ as the counterion is changed[a]

	Ground State Recovery (ps)		
	$[Fe(bpy)_3]Cl_2$	**$[Fe(bpy)_3]Br_2$**	**$[Fe(bpy)_3]I_2$**
Water	670 ± 10	675 ± 10	690 ± 15
Dimethyl Sulfoxide	800 ± 5	800 ± 10	800 ± 15
Methanol	975 ± 10	985 ± 20	995 ± 20
Acetonitrile	1020 ± 15	1015 ± 15	1015 ± 15
1-Butanol	1055 ± 15	1060 ± 20	1070 ± 10

[a]At Abs = 0.4 at the excitation wavelength.

DFT Calculations to Estimate Solvation Energy of Fe(II) Polypyridyls.

Table S3. DFT Calculations for $[Fe(bpy)_3]^{2+}$ with SMD[a] in various environments at 20 °C

	In Hartrees				
	LS E_0+G_{corr}[b]	**LS ΔG_{solv}**	**HS E_0+G_{corr}[b]**	**HS ΔG_{solv}**	**$\Delta\Delta G_{solv}$**
Vacuum	-1609.370133	-	-1609.381973	-	-
Water	-1609.565603	-0.19546982	-1609.572589	-0.19061616	-0.00485366
Dimethyl Sulfoxide	-1609.586934	-0.21680023	-1609.593817	-0.21184403	-0.00495620
Ethylene Glycol	-1609.568534	-0.19840090	-1609.574268	-0.19229524	-0.00610566
Methanol	-1609.584926	-0.21479233	-1609.590365	-0.20839209	-0.00640024
Ethanol	-1609.585110	-0.21497634	-1609.591953	-0.20998045	-0.00499589
Acetonitrile	-1609.595720	-0.22558674	-1609.603318	-0.22134551	-0.00424123
Propionitrile	-1609.596522	-0.22638842	-1609.603779	-0.22180658	-0.00458184
2-Propanol	-1609.583220	-0.21308662	-1609.588189	-0.20621647	-0.00687015
Butyronitrile	-1609.595812	-0.22567825	-1609.602916	-0.22094289	-0.00473536
1-Butanol	-1609.580662	-0.21052815	-1609.585422	-0.20344916	-0.00707899
Tetrahydrofuran	-1609.572898	-0.20276501	-1609.585249	-0.20327613	0.00051112
Diethyl Ether	-1609.554638	-0.18450457	-1609.563335	-0.18136227	-0.00314230
Dichloromethane	-1609.584294	-0.21416043	-1609.590666	-0.20869324	-0.00546719

[a]Solvent environment was applied based on the solvent list and properties built into Gaussian 09.
[b]E_0+G_{corr} refers to the sum of electronic and thermal free energies.

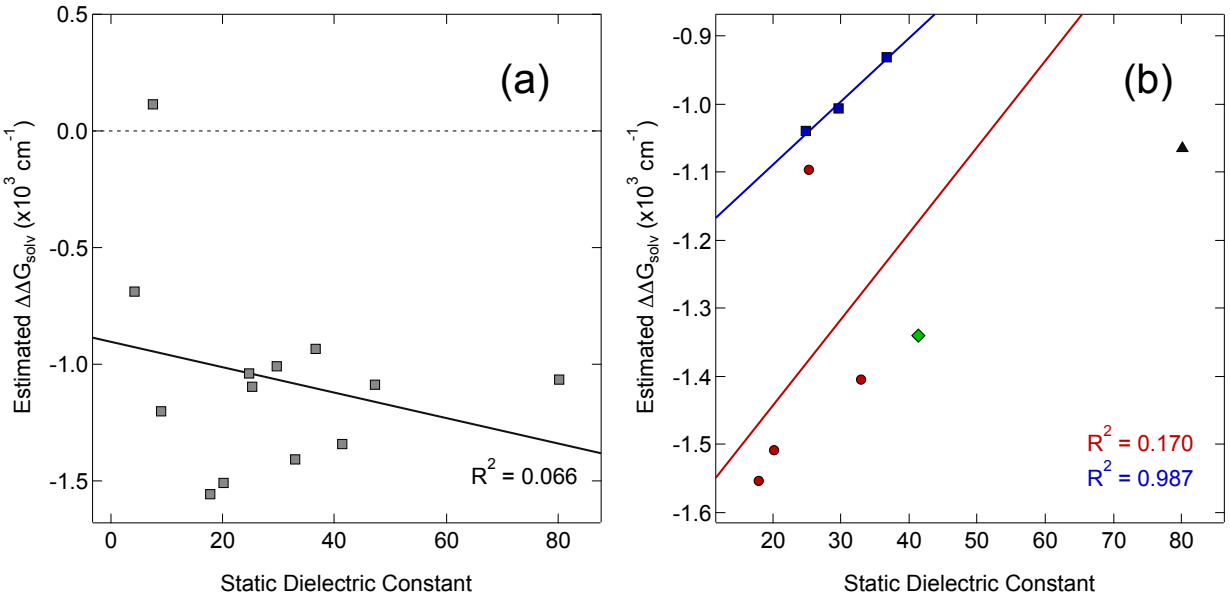

Figure S16. Correlating the static dielectric constant to the estimated differential solvation energy of $[Fe(bpy)_3]^{2+}$ from SMD calculations for (a) all solvents in this study present in the SMD solvent list and (b) a subset of the data from the left panel grouped according to solvent type, with alcohols (red circles) and nitriles (blue squares). The green diamond represents results in ethylene glycol (a diol), and the black triangle corresponds to water; neither are included in any of the fits in (b).

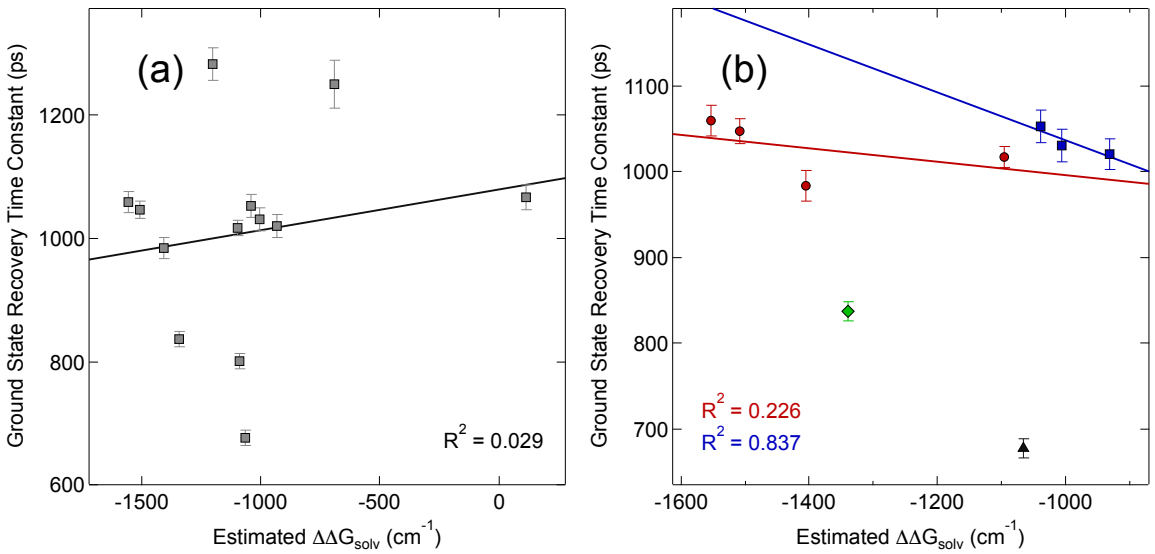

Figure S17. Correlating the estimated differential solvation energy of $[Fe(bpy)_3]^{2+}$ from SMD calculations to the associated GSR rate for (a) all solvents in this study present in the SMD solvent list and (b) a subset of the data from the left panel highlighting alcohol-based (red circles) and nitrile-based (blue squares) solvents. The green diamond represents results in ethylene glycol (a diol), and the black triangle corresponds to water; neither are included in any of the fits in (b).

Table S4. DFT Calculations for $[Fe(bpy)_3]^{2+}$ with CPCM[a] in various environments at 20 °C

	In Hartrees				
	LS E_0+G_{corr}[b]	**LS ΔG_{solv}**	**HS E_0+G_{corr}[b]**	**HS ΔG_{solv}**	**$\Delta\Delta G_{solv}$**
Vacuum	-1609.370133	-	-1609.381973	-	-
Water	-1609.262891	0.10724206	-1609.254108	0.12786517	-0.02062311
Dimethyl Sulfoxide	-1609.414762	-0.04462827	-1609.412865	-0.03089195	-0.01373632
Ethylene Glycol	-1609.395190	-0.02505665	-1609.392800	-0.01082682	-0.01422983
1,3-Propanediol	-1609.414624	-0.04449012	-1609.412790	-0.03081718	-0.01367294
1,4-Butanediol	-1609.428152	-0.05801836	-1609.426961	-0.04498854	-0.01302982
1,5-Pentanediol	-1609.436912	-0.06677828	-1609.436249	-0.05427592	-0.01250236
Propylene Carbonate	-1609.428178	-0.05804455	-1609.526835	-0.04486247	-0.01318208
Methanol	-1609.364297	0.00583626	-1609.360358	0.02161452	-0.01577826
Ethanol	-1609.396101	-0.02596743	-1609.393856	-0.01188362	-0.01408381
Acetonitrile	-1609.389014	-0.01888034	-1609.386526	-0.00455277	-0.01432757
Propionitrile	-1609.411848	-0.04171457	-1609.409954	-0.02798169	-0.01373288
2-Propanol	-1609.415117	-0.04498394	-1609.413520	-0.03154772	-0.01343622
Butyronitrile	-1609.425171	-0.05503717	-1609.423946	-0.04197296	-0.01306421
1-Butanol	-1609.425358	-0.05522423	-1609.424308	-0.04233529	-0.01288894
Tetrahydrofuran	-1609.403473	-0.03333930	-1609.402178	-0.02020512	-0.01313418
Hexanenitrile	-1609.440733	-0.07059983	-1609.440489	-0.05851666	-0.01208317
Diethyl Ether	-1609.399169	-0.02903544	-1609.398771	-0.01679824	-0.01223720
Dichloromethane	-1609.389877	-0.01974352	-1609.388043	-0.00606986	-0.01367366

[a]Solvent environment was applied under generic setting, with properties written in directly.
[b]E_0+G_{corr} refers to the sum of electronic and thermal free energies.

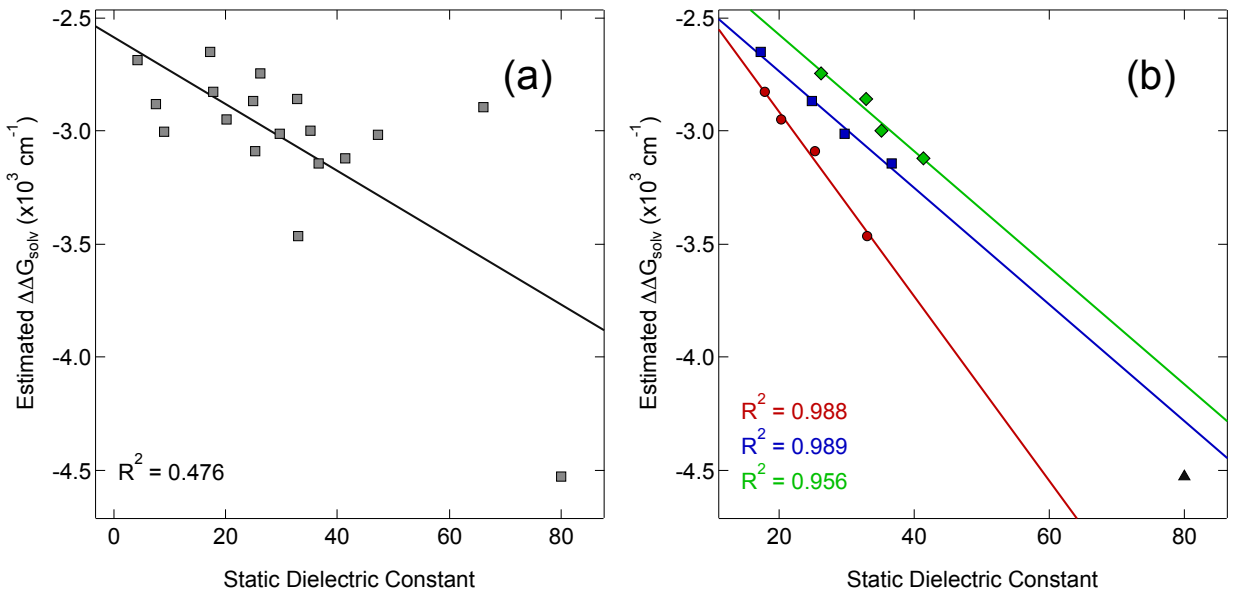

Figure S18. Correlating the static dielectric constant to the estimated change in Gibbs free energy of solvation of $[Fe(bpy)_3]^{2+}$ from CPCM calculations for (a) all solvents in this study and (b) all of the alcohol-based (red circles), diol-based (green diamonds), and nitrile-based (blue squares) solvents. The result for water (black triangle) is depicted in (b), but is not included in any of the linear fits. The data in (b) can also be found in the main text, in Figure 5a.

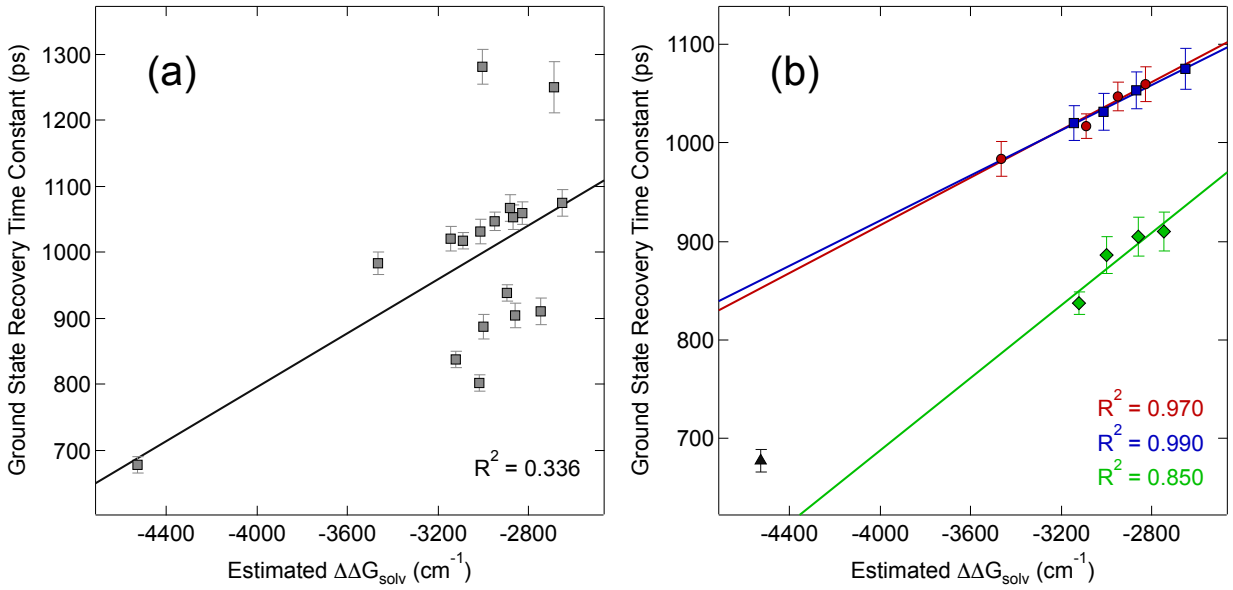

Figure S19. Correlating the estimated change in Gibbs free energy of solvation of $[Fe(bpy)_3]^{2+}$ from CPCM calculations to the associated GSR rate for (a) all solvents in this study and (b) all of the alcohol-based (red circles), diol-based (green diamonds), and nitrile-based (blue squares) solvents. The result for water (black triangle) is presented in (b), but is not included in any of the linear fits. The data in (b) can also be found in the main text, in Figure 5b.

Table S5. DFT Calculations for $[Fe(R\text{-}bpy)_3]^{2+}$ under vacuum at 20 °C

	In Hartrees	
	LS E_0+G_{corr}[a]	**HS E_0+G_{corr}[a]**
$[Fe(bpy)_3]^{2+}$	-1609.370133	-1609.381973
$[Fe(dmb)_3]^{2+}$	-1845.177892	-1845.189616
$[Fe(5,5'\text{-}dmb)_3]^{2+}$	-1845.163174	-1845.174697
$[Fe(dtbbpy)_3]^{2+}$	-2552.360790	-2552.371226

[a]E_0+G_{corr} refers to the sum of electronic and thermal free energies.

Ground State Recovery Lifetimes of $[Fe(bpy)_3]Br_2$ in Binary Solvent Systems.

Table S6. Lifetimes for $[Fe(bpy)_3]Br_2$ in water/acetonitrile solvent mixtures[a]

Percent Acetonitrile by Mass	Dielectric Constant[b]	Ground State Recovery (ps)
0	80.14	675 ± 10
25	69.71	855 ± 15
50	56.92	920 ± 10
75	46.86	965 ± 15
100	36.62	1015 ± 15

[a]At Abs = 0.4 at the excitation wavelength.

[b]Dielectric constants (at 20 °C) reported in reference 5, with 25% and 75% acetonitrile by mass values calculated by solving Equation 6 (within reference) with the parameters listed in Gagliardi et al.'s Table 2.

References

1 *CRC Handbook of Chemistry and Physics*, 98th edn.

2 M. Moosavi and A. A. Rostami, *J. Chem. Eng. Data*, 2017, **62**, 156–168.

3 P. K. Muhuri, B. Das and D. K. Hazra, *J. Chem. Eng. Data*, 1996, **41**, 1473–1476.

4 S. Mehrotra, A. Kumbharkhane and A. Chaudhari, in *Binary Polar Liquids: Structural and Dynamics Characterization Using Spectroscopic Methods*, Elsevier, 2017, pp. 215–248.

5 L. G. Gagliardi, C. B. Castells, C. Ràfols, M. Rosés and E. Bosch, *J. Chem. Eng. Data*, 2007, **52**, 1103–1107.